Flowing afterglow study of the gas phase nucleophilic reactions of some formyl, acetyl and cyclic esters

Brian T. Frink and Christopher M. Hadad *

Department of Chemistry, The Ohio State University, Columbus, OH 43210, USA.
E-mail: hadad.1@osu.edu; Fax: 614-292-1685

Received (in Cambridge, UK) 12th July 1999, Accepted 4th October 1999

A variety of nucleophiles have been investigated for their reactions with formyl and acetyl esters in the gas phase in our flowing afterglow. The reactions that are permitted in the gas phase are more varied than those seen in the condensed phase. The rates of reactions of methyl and ethyl esters as well as various lactones have been undertaken with various nucleophiles: H_2N^-, HO^-, CH_3O^-, $NCCH_2^-$, F^-, $CH_3C(=O)CH_2^-$, CH_3S^- and $O_2NCH_2^-$. For example, the reaction rate of $NCCH_2^- + HCO_2CH_2CH_3$ has been found to be $(1.3 \pm 0.2) \times 10^{-10}$ cm^3 molecule^{-1} s^{-1} and the only product is $HC(O^-)$=CHCN which results from nucleophilic acyl substitution ($B_{AC}2$) followed by a proton transfer within the ion–molecule complex. Other reaction mechanisms that have been observed include β-elimination (E2), bimolecular nucleophilic substitution at the alkyl group ($B_{AL}2$), and the Riveros reaction (elimination of CO). A mechanism for the $F^- + HCO_2CH_3$ reaction has been determined at the B3LYP/6-31+G(d) level. Most notably, channels were determined computationally ($B_{AL}2$ and Riveros), and these channels are also observed experimentally. Furthermore, the $B_{AC}2$ pathway which proceeds *via* nucleophilic attack on the carbonyl group also leads to the Riveros products, $F^-(CH_3OH)$ and CO.

Introduction

The carbonyl moiety (C=O) is fundamentally important in organic chemistry as well as in biological systems. For instance, carbonyl groups are involved in a variety of enzyme functions under aqueous conditions. The reaction pathways that occur in solution have been well examined,[1] and stabilization effects of the carbonyl group in the gas phase are reasonably well understood.[2] However, what makes carbonyl groups reactive is less well understood, and the effect of solvent (typically water) can be quite dramatic.[3] Brauman[4] and Riveros[5] have noted that many mechanistic pathways are available in the gas phase, and some of them are typically not seen in aqueous solution. By investigating reactions with carbonyl groups in the gas phase, the intrinsic reactivity of the carbonyl group can be systematically examined, and the importance of the leaving group, the nucleophilic strength, as well as the electronic and steric properties of the carbonyl group can be explored.

Previous gas phase experiments on carbonyl compounds have utilized both ion cyclotron resonance[4–6] (ICR) and flowing afterglow[6c,7] (FA) techniques. The FA has been shown to be particularly reliable in determining rate coefficients for gas phase reactions due to the presence of a bath gas (typically helium) and the moderately high pressure (typically 0.5 torr) in the reaction region. Further advancements to the FA technique include the selected ion flow tube (SIFT),[8] collision induced dissociation (CID),[9] drift capability[10] and temperature variability,[11] and these techniques have increased the role of the FA method for studying gas phase reactions. Many advantages of the flow discharge method have been elegantly reviewed by Graul and Squires.[12]

Many groups have investigated the reactivity of esters in the gas phase. Brauman,[4] Riveros[5] and their co-workers utilized ICR methods to study the reactions of various methyl esters. DePuy, Nibbering and co-workers[6c] have used both ICR and FA methods to study a number of nucleophiles for their reactions with methyl formate. Riveros and co-workers[5,13] have focussed on F^- and HO^- reactions with formyl and acetyl derivatives. Bartmess and co-workers have examined some reactions of carbanions with a variety of esters in an ICR spectrometer.[14]

The shape of the potential energy surface for gas phase reactions with carbonyl compounds has also received some experimental and computational attention. Brauman and co-workers[4] have probed the potential energy surface of $^{37}Cl^- + CF_3C(=O)^{35}Cl$ experimentally and determined that the surface contains two wells which correspond to ion–dipole complexes. Furthermore, they determined that the tetrahedral intermediate, as characterized in aqueous solution, may be a transition state or energetically inaccessible for some carbonyl reactions in the gas phase. Rice–Ramsperger–Kassel–Marcus (RRKM) transition-state theory and *ab initio* calculations provide support for the different potential energy surfaces in the gas and condensed phases.[4]

Other *ab initio* calculations have probed the factors that stabilize the carbonyl group but not the driving force for their reactivity.[2] Reactions between nucleophiles with carbonyl derivatives have been studied computationally. Jorgensen and co-workers[3] have examined nucleophilic attack at carbonyl groups (aldehydes and acid chlorides) and explored the stability of the tetrahedral intermediates.[15] Computationally, the reduction of carbonyl compounds, *i.e.* the reaction of hydride ions with typically aldehydes and ketones, has been studied[16] as well as the reactions of Cl^- with HC(=O)Cl, $CH_3C(=O)Cl$[4] and PhC(=O)Cl.[17]

A computational study of acyl transfer reactions has recently been reported by Lee and co-workers.[18] They noted that the calculated potential energy surfaces can be as simple as a single well and as complex as a triple well. They also noted that the $B_{AC}2$ mechanism is affected by the electronic preferences of the incoming nucleophile and the leaving group as well as the overall exothermicity of the reaction. These effects have also been noted experimentally.[4,5]

Some possible reactions of an anionic nucleophile with ethyl acetate are shown in Scheme 1. The pathways that are available for ethyl acetate are (a) nucleophilic acyl substitution ($B_{AC}2$), (b) proton transfer (PT) which may also be followed by fragmentation, (c) S_N2 displacement ($B_{AL}2$) which can occur on

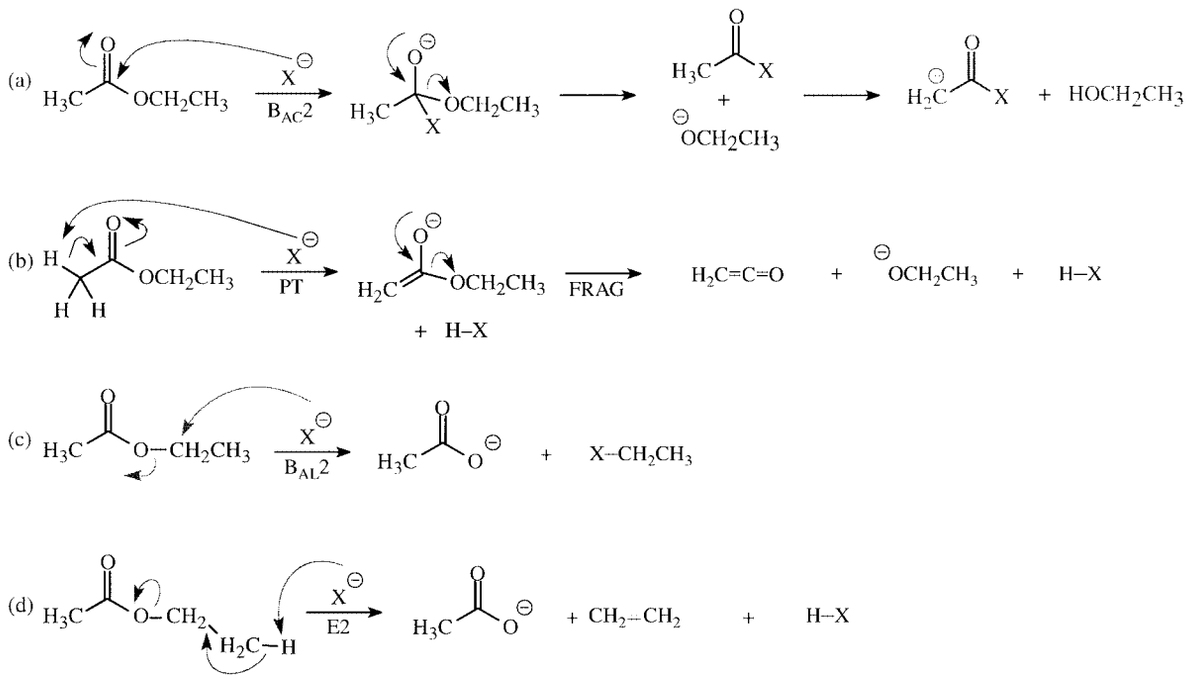

Scheme 1

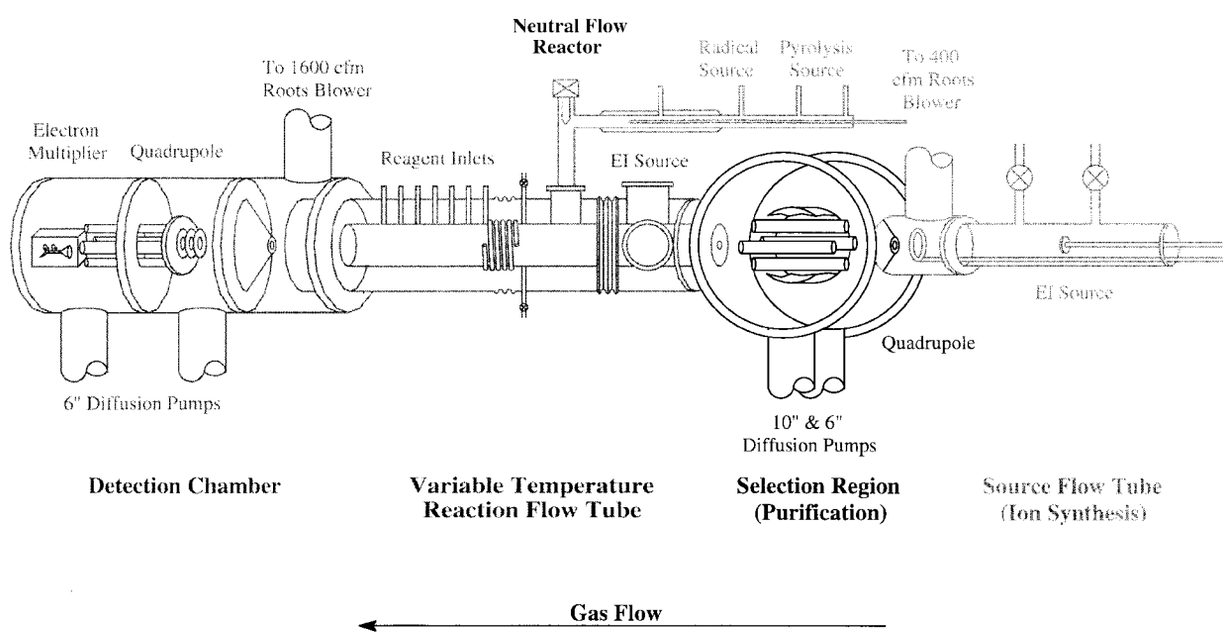

Fig. 1 A schematic diagram of our variable temperature flowing afterglow–selected ion flow tube apparatus. (Only the variable temperature flowing afterglow was used for these results.)

either alkyl group, and (d) E2 eliminations. Decarbonylation (loss of CO) is also possible for some systems and is a predominant product for formyl esters.[5] This pathway has been termed the Riveros reaction, and solvated anionic clusters are usually generated.[5]

We have completed an exhaustive study of a variety of anionic nucleophiles with formyl and acetyl esters. In addition, we present some computational results for F^- attack on methyl formate so as to understand the experimental product distribution and the mechanisms for their formation.

Experimental

These reactions were studied using a home-built variable temperature flowing afterglow (Fig. 1).[11c] Briefly, ions are generated *via* electron ionization and traverse the length (~1 m) of a stainless steel flow tube *via* a constant flow of a helium buffer gas. Neutral reagents are added downstream in order for reactions to occur, and the charged species from these reactions are subsequently monitored using quadrupole mass spectrometry. By adding these reagents at different locations along the length of the flow tube, ion–neutral reactions can be monitored as a function of distance/time, and rate coefficients can be determined.

Rate coefficients are determined under conditions of pseudo-first order kinetics, and the reported rates are averages of at least three measurements. Most of the rates reported here were obtained at 298 K and 0.5 torr, but some have been determined as a function of temperature and/or pressure.

Upon reaction with a neutral reagent, product ions can be observed. The yield of each product ion was determined by extrapolating the normalized ion percentage to the zero flow limit of the neutral reagent. This method[19] allows for the determination of primary and secondary ions. Even with this

Table 1 Rates and ionic product distributions for negative ion reactions with methyl formate (ΔH_{acid} = 391 kcal mol^{-1})[a]

Ion (A^-)	ΔH_{acid} (HA)[a]	Ionic products[b]	Rxn path	ΔH_{rxn}[c]	Rate[d]	ADO Rate[e]	Eff.[f]	Pub. rate[g]
H_2N^-	404	$HC(=O)NH^-$ (36%)	$B_{AC}2$	−38.7	19.2 ± 0.8	23.6	0.814	25.0 ± 5.0
		CH_3O^- (29%)	Riveros	−10.4				
		$CH_3O^-(NH_3)$ (24%)	Riveros					
		HCO_2^- (10%)	$B_{AL}2$					
		$CH_3O^-(CH_3OH)$ (Secondary ion)						
HO^-	391	HCO_2^- (42%)	$B_{AL}2$ or $B_{AC}2$	−38.1	17.9 ± 0.2	23.0	0.778	18.0 ± 4.0
		CH_3O^- (39%)	Riveros	4.0[h]				
		$CH_3O^-(H_2O)$ (20%)	Riveros	−20.5				
CH_3O^-	380	$CH_3O^-(CH_3OH)$ (97%)	Riveros	−17.4	8.1 ± 0.3	18.6	0.435	
		HCO_2^- (3%)	$B_{AL}2$	−35.7				
CD_3O^-	380	$CH_3O^-(CD_3OH)$ (64%)	Riveros	−17.4	10.0 ± 1.0	18.0	0.556	13.0 ± 3.0
		$CH_3O^-(CD_3OD)$ (29%)	Riveros	−17.4				
		HCO_2^- (7%)	$B_{AL}2$	−35.7				
$NCCH_2^-$	373	$HC(O^-)=CHCN$ (100%)	$B_{AC}2$		0.48 ± 0.01	17.1	0.028	0.30 ± 0.06
F^-	371	$F^-(CH_3OH)$ (57%)	Riveros	−9.7	21.0 ± 2.0	22.1	0.950	
		HCO_2^- (43%)	$B_{AL}2$	−19.4				
$CH_3C(=O)CH_2^-$	369	$CH_3C(=O)CH_2^-(CH_3OH)$ (60%)	Riveros		0.09 ± 0.01	15.5	0.006	
		HCO_2^- (40%)	$B_{AL}2$	−33.4				
CH_3S^-	357	HCO_2^- (95%)	$B_{AL}2$	−19.4				
		$CH_3S^-(CH_3OH)$ (5%)	Riveros					
$O_2NCH_2^-$	356	HCO_2^- (66%)	$B_{AL}2$		0.07 ± 0.01	15.3	0.005	
		$O_2NCH_2^-(CH_3OH)$ (34%)	Riveros					

[a] Values from the NIST website (http://webbook.nist.gov). [b] %Yields are extrapolated for a zero flow rate of neutral reagent in STP cm^3 s^{-1}. [c] ΔH_{rxn} in kcal mol^{-1}, calculated from values reported by NIST (http://webbook.nist.gov). [d] Rates in units of (10^{-10} cm^3 molecule^{-1} s^{-1}) and the reported errors are one standard deviation of at least triplicate measurements. [e] Rates in units of (10^{-10} cm^3 molecule^{-1} s^{-1}) and the polarizability for HCO_2CH_3 is approximated using group additivity. [f] Efficiency = (experimental rate/ADO rate). [g] Reference 6*c*, in units of 10^{-10} cm^3 molecule^{-1} s^{-1}. [h] The ΔH_{rxn} assumes H_2O and CO as products. If HCO_2H was a product, ΔH_{rxn} would be −2.3 kcal mol^{-1}, but PT should have also occurred.

extrapolation, the accuracy of the product determination should be considered as ±10%.[19] These percent yields are taken as the average of three different initial flow rates of the neutral reagent where each is extrapolated to the zero flow limit of the neutral compound.

In this work, the helium (Praxair, ≥99.995%) bath gas is further purified by passing the gas through a copper coil, packed with 4 Å molecular sieves, that is submerged in liquid nitrogen. The purified helium is then passed over the filament of the EI source. H_2N^- is then formed from electron ionization of NH_3 (AGA, 99.99%). There is always some impurity of HO^- when H_2N^- is generated in our system (as is typical for flowing afterglows), but in the experiments reported here, the ratio of H_2N^- to HO^- was always better than 9 : 1, and a correction for the presence of HO^- was not performed.

For some experiments, H_2N^- was used to deprotonate H_2O for generating HO^-, but on most occasions, HO^- was generated by dissociative electron attachment on N_2O (AGA, 99.5%), followed by hydrogen atom abstraction from CH_4 (AGA, 99.99%). HO^- or H_2N^- was subsequently used to deprotonate CH_3OH (Fisher, 99.9%), CD_3OD (Cambridge Isotopes, 99.8%), CH_3CN (Mallinckrodt, 99.9%), $CH_3C(=O)CH_3$ (Mallinckrodt, 99.8%), and CH_3NO_2 (Aldrich, 96%) to form CH_3O^-, CD_3O^-, $NCCH_2^-$, $CH_3C(=O)CH_2^-$, and $O_2NCH_2^-$, respectively. The reaction of HO^- with CH_3SSCH_3 (Aldrich, 98%) generated CH_3S^-. Finally, F^- was formed by electron ionization of NF_3 (Air Products, 99.5%). These compounds were used as provided by the manufacturer. The neutral reagents, HCO_2CH_3 (Aldrich, 97%), $HCO_2CH_2CH_3$ (Baker, 98.1%), $CH_3CO_2CH_3$ (Aldrich, 99+%), $CH_3CO_2CH_2CH_3$ (Mallinckrodt, 99.9%), β-propiolactone (Acros, 98%), and γ-butyrolactone (Acros, 99+%), were used as provided by the commercial sources.

Computational methods

All calculations were performed with the GAUSSIAN94 suite of programs.[20] All stationary points were fully optimized at the B3LYP/6-31+G* level[21] of theory and confirmed as minima or transition states *via* vibrational frequency analysis calculations. All transition states were confirmed to have only one imaginary vibrational frequency. The reactant and product which connected each transition state was confirmed by an intrinsic reaction coordinate[22] (IRC) search or by incremental (typically 10%) displacement along the vibrational mode for the imaginary frequency and then a careful optimization (opt = calcfc or calcall) in either direction. All energies reported here include (unscaled) zero point vibrational energy and thermal corrections to 298 K (1 atm pressure).

Results

Rate coefficients have been determined for the reactions of H_2N^-, HO^-, CD_3O^-, $NCCH_2^-$, F^-, $CH_3C(=O)CH_2^-$, and $O_2NCH_2^-$ with methyl formate and methyl acetate. For reactions with ethyl formate and ethyl acetate, only H_2N^-, HO^-, CH_3O^-, $NCCH_2^-$, F^-, and $O_2NCH_2^-$ were used. The reactivity of these esters is compared to β-propiolactone and γ-butyrolactone in order to examine acyclic *vs*. cyclic esters.

General trends

The rate coefficients for the reactions of H_2N^-, HO^-, CH_3O^- or CD_3O^-, and F^- with all of the esters have been found to be near the theoretical Average Dipole Orientation (ADO) rate limit (1.5 to 2.5 × 10^{-9} cm^3 molecule^{-1} s^{-1} for these systems). However, the rate coefficients with $NCCH_2^-$, $CH_3C(=O)CH_2^-$, and $O_2NCH_2^-$ are much less efficient with rates between 10^{-10} to 10^{-12} cm^3 molecule^{-1} s^{-1}, as seen in Table 1.

For example, the reaction rates for H_2N^- with methyl formate, ethyl formate, methyl acetate, and ethyl acetate are (19.2 ± 0.8), (28 ± 1), (26 ± 2), and (33 ± 5) × 10^{-10} cm^3 molecule^{-1} s^{-1}, and the efficiencies[23] (k_{OBS}/k_{ADO}) of these reactions are quite high (Tables 1–4). When comparing the rates and efficiencies for the formate and acetate esters, the ethyl esters seem to react faster and more efficiently. This trend appears to be independent of the chosen nucleophile (except $O_2NCH_2^-$ which does not react with the ethyl esters). Thus, the alkyl group of the ester has an important role in the rate of reaction. This is most probably due to the different reaction pathways that are available to the various esters (see below).

Table 2 Rates and ionic product distributions for negative ion reactions with ethyl formate

Ion (A^-)	ΔH_{acid} (HA)[a]	Ionic products[b]	Rxn path	ΔH_{rxn}[c]	Rate[d]	ADO Rate[e]	Eff.[f]
H_2N^-	404	HCO_2^- (or $CH_3CH_2O^-$) (72%)	E2 or $B_{AL}2$ (or Riveros)	−41.1 or —[g] (or −13.1)	28.0 ± 1.0	27.2	1.00
		$HC(=O)NH^-$ (26%)	$B_{AC}2$	−38.3			
		$CH_3CH_2O^-(NH_3)$ (3%)	Riveros				
HO^-	391	HCO_2^- (95%)	E2 or $B_{AL}2$ or $B_{AC}2$	−26.7 or −37.7 or −37.7	27.0 ± 1.0	26.5	1.00
		$CH_3CH_2O^-(H_2O)$ (5%)	Riveros				
CH_3O^-	380	HCO_2^- (or $CH_3CH_2O^-$) (53%)	E2 or $B_{AL}2$ (or $B_{AC}2$)	−18.6 or −34.8 (or −2.7)	19.0 ± 2.0	21.1	0.90
		$CH_3CH_2O^-(CH_3OH)$ (47%)	Riveros				
$NCCH_2^-$	373	$HC(O^-)=CHCN$ (100%)	$B_{AC}2$		1.3 ± 0.2	19.3	0.07
F^-	371	HCO_2^- (or $CH_3CH_2O^-$) (79%)	E2 or $B_{AL}2$ (or $B_{AC}2$)	−7.5 or −29.7 (or +22.2)	36.0 ± 6.0	25.4	1.00
		$F^-(CH_3CH_2OH)$ (21%)	Riveros				
$O_2NCH_2^-$	356	HCO_2^- (100%)	E2 or $B_{AL}2$	+4.4 or —[g]	0.06 ± 0.01	17.1	0.004

[a] Values from the NIST website (http://webbook.nist.gov). [b] %Yields are extrapolated for a zero flow rate of neutral reagent in STP $cm^3\ s^{-1}$. [c] ΔH_{rxn}, in kcal mol^{-1}, calculated from values reported by NIST (http://webbook.nist.gov). [d] Rates in units of (10^{-10} cm^3 $molecule^{-1}$ s^{-1}) and the reported errors are one standard deviation of at least triplicate measurements. [e] Rates in units of (10^{-10} cm^3 $molecule^{-1}$ s^{-1}). [f] Efficiency = (experimental rate/ADO rate), and limited to a value of 1. [g] Experimental values are not available.

Table 3 Rates and ionic product distributions for negative ion reactions of methyl acetate (ΔH_{acid} = 372 kcal mol^{-1})[a]

Ion (A^-)	ΔH_{acid} (HA)[a]	Ionic products[b]	Rxn path	ΔH_{rxn}[c]	Rate[d]	ADO Rate[e]	Eff.[f]	Pub. rate[e]
H_2N^-	404	$(M–H)^-$ (≥99%)	PT	−32.0	26.0 ± 2.0	24.5	1.00	
		$CH_3C(=O)NH^-$ (≤1%)	$B_{AC}2$	−37.6				
HO^-	391	$CH_3CO_2^-$ (78%)	$B_{AL}2$ or $B_{AC}2$	−36.7	28.0 ± 2.0	23.9	1.00	
		$(M–H)^-$ (22%)	PT	−19.0				
CD_3O^-	380	$(M–H)^-$ (100%)	PT	−8.0	15.1 ± 0.7	18.4	0.82	
$NCCH_2^-$	373	$(M–H)^-$ (57%)	PT	−1.0	0.37 ± 0.02	17.5	0.02	
		$CH_3C(O^-)=CHCN$ (43%)	$B_{AC}2$					
F^-	371	$FC(=O)CH_2^-$ (36%)	$B_{AC}2$ + PT		28.0 ± 1.0	22.9	1.00	2.2[g]
		$CH_3CO_2^-$ (21%)	$B_{AL}2$	−18.0				
		$F^-(CH_3OH)$ (14%)	$B_{AC}2$ + E2					
		$(M–H)^-$ (14%)	PT	1.0				
		$F^-(CH_3CO_2CH_3)$ (14%)	Adduct					
$CH_3C(=O)CH_2^-$	369	No observed reaction				15.7		
$O_2NCH_2^-$	356	No observed reaction				15.5		

[a] Values from the NIST website (http://webbook.nist.gov). [b] %Yields are extrapolated for a zero flow rate of neutral reagent in STP $cm^3\ s^{-1}$. [c] ΔH_{rxn}, in kcal mol^{-1}, calculated from values reported by NIST (http://webbook.nist.gov). [d] Rates are in units of (10^{-10} cm^3 $molecule^{-1}$ s^{-1}) and the reported errors are one standard deviation of at least triplicate measurements. [e] Rates are in units of (10^{-10} cm^3 $molecule^{-1}$ s^{-1}). [f] Efficiency = (experimental rate/ADO rate), and limited to a value of 1. [g] Reference 27.

Table 4 Rates and ionic product distributions for negative ion reactions with ethyl acetate

Ion (A^-)	ΔH_{acid} (HA)[a]	Ionic products[b]	Rxn path	ΔH_{rxn}[c]	Rate[d]	ADO Rate[e]	Eff.[f]	Pub. rate[e]
H_2N^-	404	$(M–H)^-$ (64%)	PT		33.0 ± 5.0	27.2	1.00	
		$CH_3CO_2^-$ (31%)	E2 or $B_{AL}2$	−40.0 or —[g]				
		$CH_3C(=O)NH^-$ (5%)	$B_{AC}2$	−37.5				
HO^-	391	$CH_3CO_2^-$ (68%)	$B_{AC}2$ or E2 or $B_{AL}2$	−36.6 or −25.6 or −36.6	24.0 ± 1.0	26.5	0.91	
		$(M–H)^-$ (32%)	PT					
CH_3O^-	380	$(M–H)^-$ (83%)	PT		19.1 ± 0.1	20.9	0.91	
		$CH_3CO_2^-$ (17%)	E2 or $B_{AL}2$	−17.5 or −33.7				
$NCCH_2^-$	373	$CH_3C(O^-)=CHCN$ (53%)	$B_{AC}2$		0.41 ± 0.1	19.1	0.02	
		$(M–H)^-$ (47%)	PT					
F^-	371	$FC(=O)CH_2^-$ (54%)	$B_{AC}2$ + PT		35.0 ± 8.0	25.3	1.00	2.1[h]
		$CH_3CO_2^-$ (46%)	E2 or $B_{AL}2$	−6.5 or —[g]				
$O_2NCH_2^-$	356	No observed reaction				16.7		

[a] Values from the NIST website (http://webbook.nist.gov). [b] %Yields are extrapolated for a zero flow rate of neutral reagent in STP $cm^3\ s^{-1}$. [c] ΔH_{rxn}, in kcal mol^{-1}, calculated from values reported by NIST (http://webbook.nist.gov). [d] Rates are in units of (10^{-10} cm^3 $molecule^{-1}$ s^{-1}) and the reported errors are one standard deviation of at least triplicate measurements. [e] Rates are in units of (10^{-10} cm^3 $molecule^{-1}$ s^{-1}). [f] Efficiency = (experimental rate/ADO rate), and limited to a value of 1. [g] Experimental data are not available. [h] Reference 27.

However, $NCCH_2^-$ reacts exclusively with formate esters *via* a $B_{AC}2$ mechanism to yield $HC(O^-)=CHCN$ and the corresponding alcohol (Tables 1 and 2) and undergoes $B_{AC}2$ or proton transfer reactions with acetate esters (Tables 3 and 4). This is the one example where the products of the reaction seem to be driven entirely by the nucleophile. Plots of the Riveros product yields for the formyl esters and the proton transfer yields for the acetyl esters for the different nucleophiles are shown in Fig. 2, and these will be discussed further below.

Not only are the ethyl esters more reactive, based on the rate coefficients, but they also yield a larger percentage of products from the reaction at the alkyl group than at the carbonyl group. If the ethyl esters were undergoing $B_{AL}2$ reactions, like the

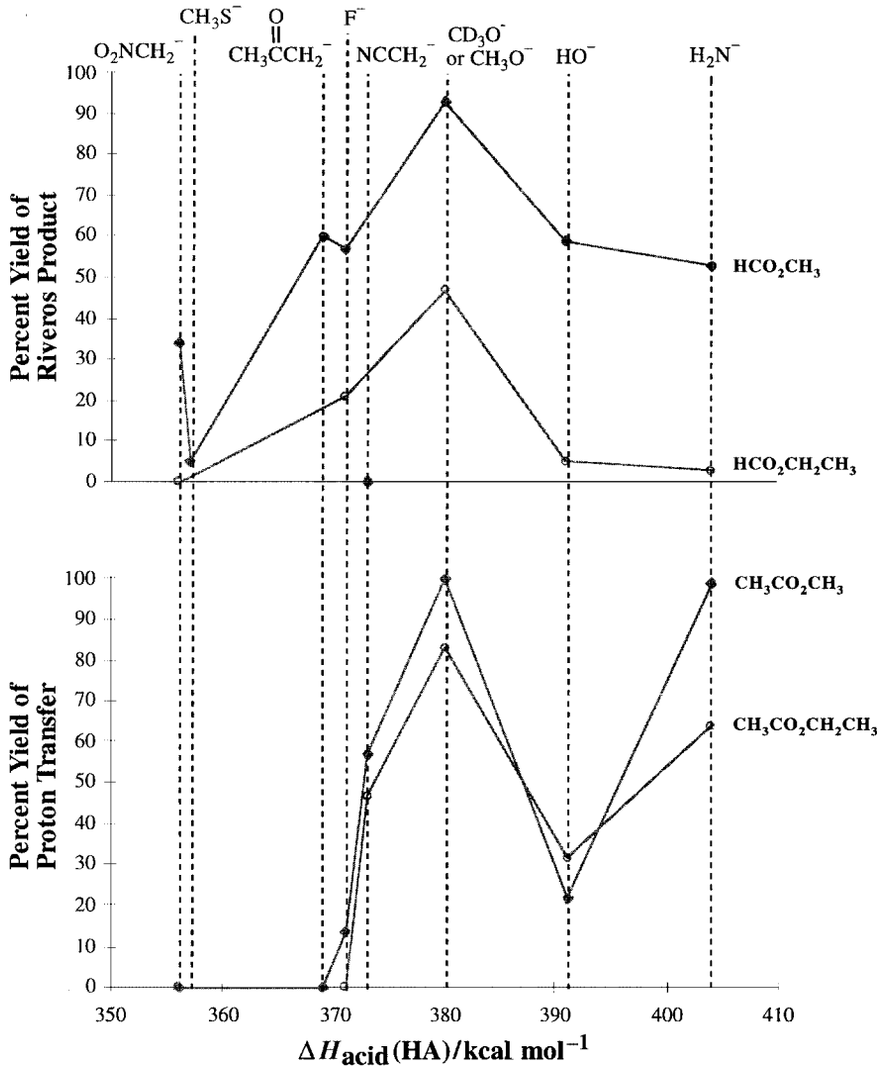

Fig. 2 Correlation of the Riveros product yields for the formyl esters and the proton transfer yields for the acetyl esters for the different nucleophiles according to their gas phase acidity (ΔH_{acid}).

methyl esters, the reactions should be slower due to increased steric congestion.[24] In addition, the methylene carbon should be less electrophilic as the methyl group is generally considered to be electron-donating/polarizable as compared to a hydrogen atom. Both of these would cause the reaction to slow down, yet the reaction rate increases. Therefore, the formation of the carboxylate ion in the alkyl esters occurs predominantly *via* an elimination (E2) rather than a nucleophilic substitution ($B_{AL}2$) pathway (Scheme 1). These aspects are similar to those discussed by DePuy, Bierbaum and co-workers in their pioneering studies of the factors that favor elimination *vs*. substitution mechanisms in alkyl halides and other organic compounds.[24,25]

Reactions of methyl formate

The product ions observed from nucleophilic attack on methyl formate can be used to infer the mechanistic pathways that generated these product ions. For the H_2N^- + HCO_2CH_3 reaction in our FA, four primary products, $HC(=O)NH^-$ (36%), CH_3O^- (29%), $CH_3O^-(NH_3)$ (24%) and HCO_2^- (10%), and one secondary product $CH_3O^-(CH_3OH)$ are generated (Table 1). These products and their approximate yields are in reasonable agreement with results by DePuy and co-workers,[6c] except that we do not detect the formation of the $(M–H)^-$ anion from the formyl derivatives. As noted by DePuy and co-workers, such $(M–H)^-$ anions will react with excess neutral reagents from the ionization source of the flowing afterglow (such as NH_3 used to generate H_2N^-) and will yield additional products. Therefore, our FA product yields should be considered as qualitative for the formate esters.

A typical spectrum of H_2N^- + HCO_2CH_3 as well as the extrapolation to zero methyl formate flow (so as to obtain the product yields) are shown in Fig. 3. As stated above, the extrapolation procedure should provide qualitative information about the primary products of these reactions. As seen in Fig. 3, the presence of the $HC(=O)NH^-$ product demonstrates that there is sufficient time and energy for proton transfer to occur between CH_3O^- and $HC(=O)NH_2$ in the ion–molecule complex during the $B_{AC}2$ pathway. Therefore, a tetrahedral species is accessible for this reaction.

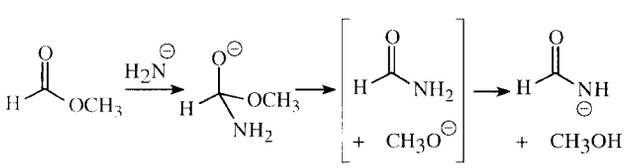

The methoxide ion product is most likely generated *via* a Riveros (decarbonylation) reaction since the $HC(=O)NH^-$ ion is also observed (see below). The $CH_3O^-(NH_3)$ complex is definitely formed *via* a Riveros (decarbonylation) reaction. The formate ion is generated *via* a $B_{AL}2$ mechanism, and attack on the methyl group of the ester results in formation of methylamine as a neutral (and undetected) product.

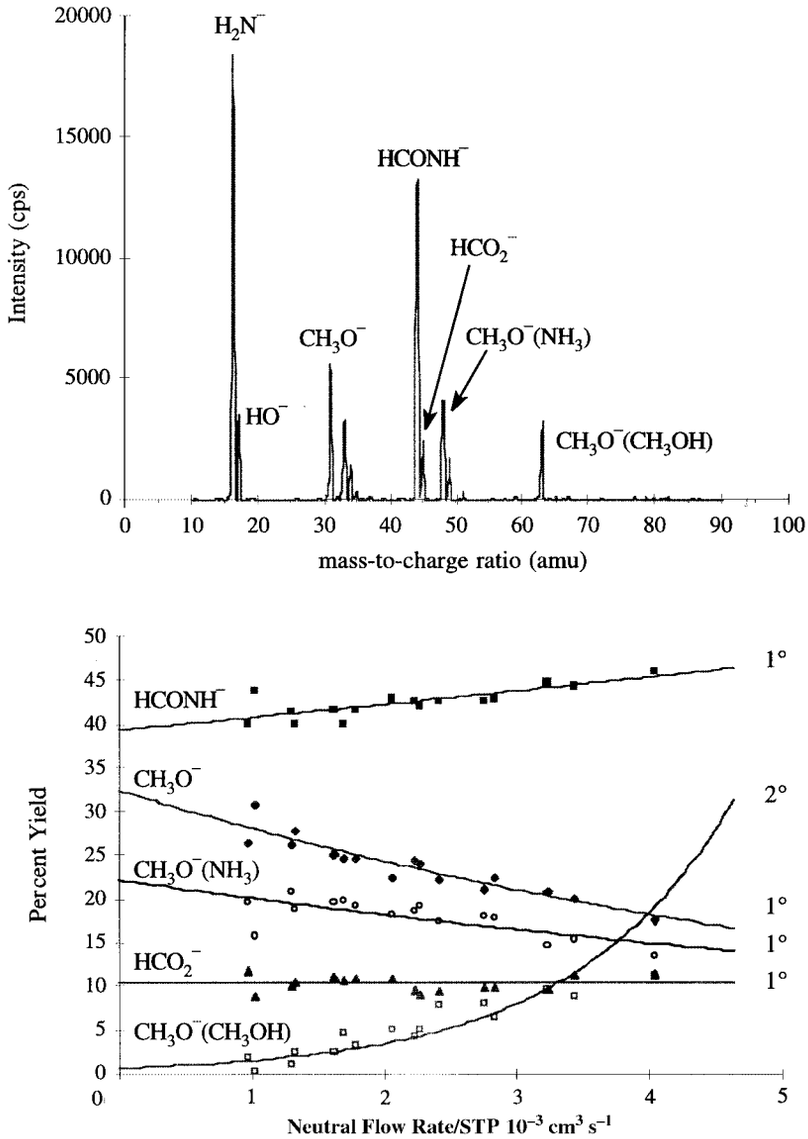

Fig. 3 A typical spectrum (0.5 torr and 298 K) for the reaction of H_2N^- with methyl formate (HCO_2CH_3) at the longest reaction time (top), and extrapolation to zero flow of methyl formate for determining the primary products of this reaction (bottom).

The reaction of HO^- ion with methyl formate produces HCO_2^- (42%), CH_3O^- (39%), and $CH_3O^-(H_2O)$ (20%). Again, the reaction agrees with results by DePuy and co-workers,[6c] except that the $(M–H)^-$ ion is not detected in our FA due to subsequent reactions. Both the methoxide ion and the methoxide ion–water complex products are formed from the Riveros reaction. The methoxide ion could be generated *via* a $B_{AC}2$ reaction, but the formic acid product would transfer a proton (like formamide, above) to the methoxide ion to produce the more stable methanol and formate ion. The formate ion can be formed *via* a $B_{AC}2$ pathway (after a proton transfer in the ion–molecule complex) or from $B_{AL}2$ attack upon the methyl group of methyl formate. The efficiency of the HO^- reaction with methyl formate reaction was 79%, while the reaction with amide ion was 81%.

The reaction of CH_3O^- and CD_3O^- with methyl formate yields HCO_2^- resulting from the $B_{AL}2$ pathway in small percentages (3 and 7%, respectively). The other products observed are complexes of methoxide ion with methanol (protiated or deuterated) which result from a Riveros reaction. We observed two different complexes as the original deuterated methoxide was generated from the reaction of HO^- (or H_2N^-) with CD_3-OD, and some H/D exchange could have occurred. In previous ICR experiments by Riveros and co-workers,[5] the naked methoxide ion was also observed as a product. However, we do not observe this ionic product, and this is in agreement with previous FA results by DePuy and co-workers.[6c] Therefore, the formation of the methoxide ion may be due to the low pressures in which the ICR experiments were conducted.

The remainder of the ions, excluding $NCCH_2^-$ which was mentioned previously, follow the same pattern as methoxide ion. A Riveros product is formed as a complex between methanol and the reactant ion, and HCO_2^- is formed as another product *via* a $B_{AL}2$ reaction. The Riveros products are dominant for both F^- and $CH_3C(=O)CH_2^-$, while the Riveros pathway is the minor channel for CH_3S^- and $O_2NCH_2^-$. In fact, the Riveros reaction is the favored pathway for the less basic ions (A^-) with a $\Delta H_{acid}(HA) \geq 369$ kcal mol^{-1} (Table 1), neglecting $NCCH_2^-$ where only the $B_{AC}2$ pathway is observed as noted earlier.

We also examined the Riveros reaction of $NCCH_2^-$ with methyl formate as a function of temperature from 298 to 448 K, in 50 K increments (Table 5). The reaction shows a negative temperature dependence, and the only product observed at all temperatures is $HC(O^-)=CHCN$ (*via* a $B_{AC}2$ mechanism followed by a proton transfer).

Experimentally, the reaction of F^- with HCO_2CH_3 occurs with 95% efficiency and yields $F^-(CH_3OH)$ (Riveros) and HCO_2^- ($B_{AL}2$) products. A representative spectrum (at 298 K for a long reaction time) is shown in Fig. 4. The reaction occurs

Table 5 Variable temperature studies at 0.5 torr

Reaction	Rate[a]/10^{-10} cm^3 molecule^{-1} s^{-1}				Products	Mechanistic pathway	Product distribution (%)[b]			
	298 K	348 K	398 K	448 K			298 K	348 K	398 K	448 K
$F^- + HCO_2CH_3$	21.0 ± 2.0	27.2 ± 0.4	26.0 ± 1.0	21.0 ± 3.0	HCO_2^-	$B_{AL}2$	43	18	15	6
					$F^-(CH_3OH)$	Riveros	57	82	85	94
$F^- + CH_3CO_2CH_3$	28.0 ± 1.0	29.0 ± 4.0	31.0 ± 2.0	29.0 ± 5.0	$F^-(CH_3OH)$	$B_{AC}2$ + E2	14	9	5	10
					$CH_3CO_2^-$	$B_{AL}2$	21	13	12	11
					$FC(=O)CH_2^-$	$B_{AC}2$ + PT	36	70	65	74
					$(M–H)^-$	PT	14	6	16	15
					$F^-(CH_3CO_2CH_3)$	Adduct	14	3	1	0
$NCCH_2^- + HCO_2CH_3$	0.48 ± 0.01	0.38 ± 0.01	0.23 ± 0.01	0.15 ± 0.02	$HC(O^-)=CHCN$	$B_{AC}2$	100	100	100	100

[a] Reported errors are one standard deviation of at least triplicate measurements. [b] Product distributions for four different temperatures.

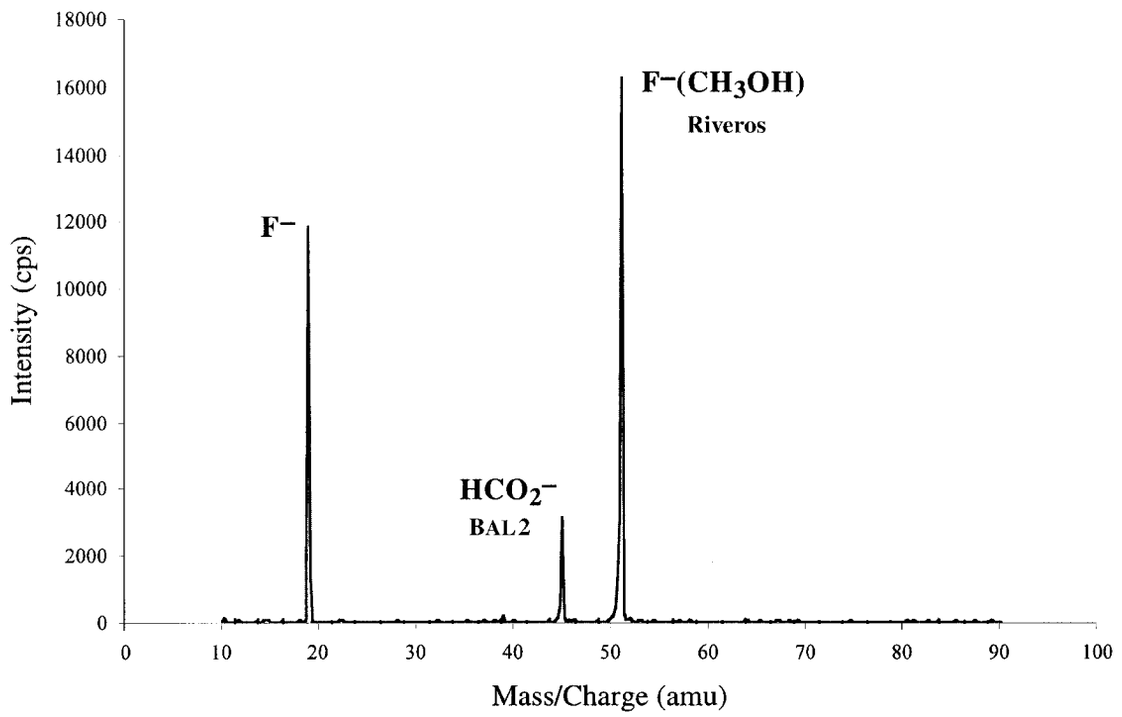

Fig. 4 A typical spectrum for the reaction of F^- with methyl formate (HCO_2CH_3) at 0.5 torr and 298 K at our longest reaction time. (The extrapolation of the product's intensities to the zero flow limit provides the data shown in Table 5.)

upon almost every collision, and the Riveros product is favored at 298 K after extrapolation to zero neutral flow of methyl formate (Table 5). Therefore, despite the larger exothermicity (calculated at the B3LYP/6-31+G(d) level) of the $B_{AL}2$ reaction ($\Delta H_{rxn} = -24.1$ kcal mol^{-1}), the Riveros pathway ($\Delta H_{rxn} = -12.9$ kcal mol^{-1}) dominates.

The origin of this preference is of interest. We, therefore, calculated the entire potential energy surface for $F^- + HCO_2CH_3$ at the B3LYP/6-31+G(d) level. These enthalpy results (in kcal mol^{-1} at 298 K) are presented in Fig. 5, and the relative enthalpy of the $F^- + HCO_2CH_3$ reactants is set at zero. The pathway for the $B_{AL}2$ process (Fig. 5a) proceeds through an ion–dipole complex that is −14.2 kcal mol^{-1} more stable than the reactants at infinite separation. The transition state for cleavage of the O–CH_3 bond is 4.3 kcal mol^{-1} higher in energy than the complex, but still exothermic relative to the reactants. The Riveros reaction could possibly occur *via* direct attack of F^- on the formyl hydrogen (Fig. 5b), and DePuy, Nibbering and co-workers[6c] have cited the large complexation energy as a driving force for this process. The direct proton abstraction pathway for the Riveros reaction was exhaustively searched for without success; however, a transition state for deprotonation concomitant with C–O cleavage was located which yields the $F^-(CH_3OH)$ complex along with dissociated CO. This transition state is +0.3 kcal mol^{-1} higher in energy than the reactants, but proceeds through a more stable ion–dipole complex (by ~4 kcal mol^{-1}) relative to the $B_{AL}2$ pathway. Thus, the relative activation barriers would suggest that the $B_{AL}2$ pathway should strongly dominate at 298 K, but experimentally, we observe a 57 : 43 preference for Riveros : $B_{AL}2$. These results suggest that either the B3LYP/6-31+G(d) method underestimates the energy barriers in this system or some dynamical effects are also important due to the differences in the energies of the ion–dipole complexes.

We also searched for the process by which nucleophilic acyl substitution (NAS, $B_{AC}2$) would proceed. Coordination of F^- to methyl formate leads to a doubly-bridged ion–dipole complex where the (normally less stable) *E* conformation of the ester is involved. This ion–dipole complex is the most stable (−22.1 kcal mol^{-1} relative to reactants) of the complexes located. Formation of a tetrahedral intermediate is achieved *via* a relatively low energy transition state; however, the endothermic (+5.2 kcal mol^{-1}) transition state for C–OCH_3 bond cleavage leads directly to deprotonation of the formyl hydrogen by CH_3O^- upon departure. Subsequent fragmentation of FCO^- within the $FCO^-(CH_3OH)$ complex then leads to the $F^-(CH_3OH)$ complex. Thus, the process of nucleophilic attack at the carbonyl carbon also leads to formation of the Riveros

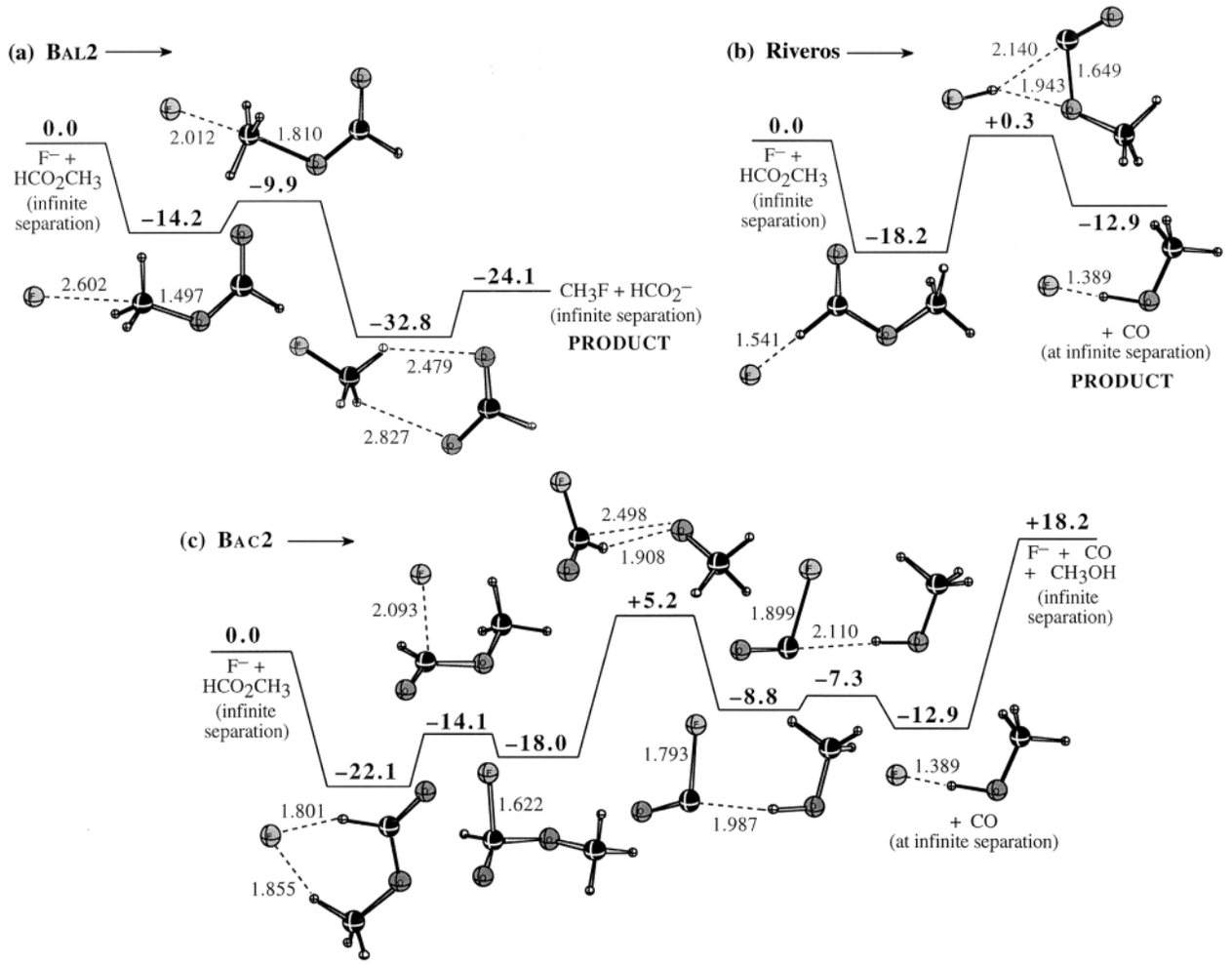

Fig. 5 Potential energy surface for the reaction of F^- with methyl formate (HCO_2CH_3) as calculated at the B3LYP/6-31+G* level (ΔH in kcal mol^{-1} at 298 K). Selected bond distances are shown in Å.

products as the basicity of CH_3O^- drives the final proton transfer.

The transition states for the cleavage of the C–OCH_3 bond, either in the Riveros pathway (Fig. 5b) or the $B_{AC}2$ pathway (Fig. 5c), have a barrier that is larger than the energy of the initial F^- and HCO_2CH_3. Therefore, an increase in internal energy (temperature) might be able to favor the Riveros reaction. Experimentally, the reaction of F^- with methyl formate at room temperature (Table 5) produces $F^-(CH_3OH)$, the Riveros product, in 57% yield and HCO_2^-, the $B_{AL}2$ product, in 43% yield. The percent yield (57, 82, 85, and 94%) of the Riveros reaction increases with increasing temperature (298, 348, 398, and 448 K, respectively) as predicted by the barrier seen in the calculated potential energy surface (Fig. 5). Of course, this is a very simple analysis, and temperature effects on the potential energy surface will be important for both reaction channels.

Reactions of ethyl formate

As with methyl formate, the reaction of $NCCH_2^-$ with ethyl formate is unique and generates only a $B_{AC}2$ product (HC(=O)-$CHCN^-$). For most of the anionic reactions with ethyl formate, the Riveros reaction is the minor pathway for reaction. As stated earlier, the reaction at the alkyl group is most likely to occur *via* an E2 elimination, but the possibility of $B_{AL}2$ has not been conclusively eliminated. However, the fast reaction rates and the high efficiencies of the ethyl formate reactions suggest that a new pathway is dominant. We believe that this new pathway is an E2 elimination and is in agreement with previous results by Riveros and co-workers.[5] For the reaction with ethyl formate, the formate and ethoxide ions cannot be distinguished in our system as our instrument only has unit mass resolution. However, in analogy to the acetyl ester reactions (see below) where this isobaric situation may not occur for acetate *vs.* ethoxide ions, we are confident that HCO_2^- is the dominant ion for the reactions with ethyl formate. (Recent experiments with $H^{18}O^-$ as a nucleophile also confirm these conclusions.[26])

For H_2N^- with ethyl formate, the products are very similar to those in the case of methyl formate. The products are HCO_2^- and/or $CH_3CH_2O^-$ (72%), $HC(=O)NH^-$ (26%), and $CH_3CH_2O^-(NH_3)$ (3%). The mechanisms that would lead to the formation of these product ions are E2 and/or Riveros, $B_{AC}2$, and the Riveros pathways, respectively.

Similar reactivity is seen for HO^-. The products, as in the reaction with methyl formate, are HCO_2^- and/or $CH_3CH_2O^-$ (95%) and $CH_3CH_2O^-(H_2O)$ (5%). The pathways involved are E2 and/or $B_{AC}2$ for the formation of HCO_2^-, and the Riveros reaction would form $CH_3CH_2O^-$ and the $CH_3CH_2O^-(H_2O)$ complex.

For the reaction of methoxide ion with ethyl formate, the products are HCO_2^- and/or $CH_3CH_2O^-$ (53%) and CH_3-$CH_2O^-(CH_3OH)$ (47%). Since CH_3O^- was not generated in the reaction with CD_3O^- with methyl formate, the amount of $CH_3CH_2O^-$ generated from the reaction with ethyl formate is likely to be negligible. Also, the true yield of the Riveros reaction can be assigned to the $CH_3CH_2O^-(CH_3OH)$ complex. In this case, the Riveros pathway only accounts for 47% of the reaction, while the E2 reaction accounts for about 53%.

The reaction of F^- with ethyl formate yields HCO_2^- (79%) and $F^-(CH_3CH_2OH)$ (21%). Here, we have once again reasoned by analogy and discounted the possibility of $CH_3CH_2O^-$ as a possible product ion because this F^- reaction seems to compare

very well to the methyl formate case. The ethyl formate reaction favors E2 (79%) over decarbonylation (21%).

With $O_2NCH_2^-$ and ethyl formate, the Riveros product is not seen. The reaction is very slow [$(6 \pm 1) \times 10^{-12}$ cm^3 molecule^{-1} s^{-1}] and yields HCO_2^- as the only product. It appears that the reaction proceeds exclusively *via* a $B_{AL}2$ reaction at the alkyl group.

Reactions with methyl acetate

In the reactions with methyl acetate (ΔH_{acid} = 372 kcal mol^{-1}), the noticeable trend is that proton transfer is the favored pathway for this ester with all nucleophiles/bases considered here except HO^- and F^- ions. Furthermore, $CH_3C(=O)CH_2^-$ and $O_2NCH_2^-$ were unreactive on the time scale of our experiments. Table 3 lists all of the products and rate coefficients for the reactions with methyl acetate.

The reaction of H_2N^- proceeds at a rate of $(26 \pm 2) \times 10^{-10}$ cm^3 molecule^{-1} s^{-1} and produces ≤1% of $CH_3C(=O)NH^-$ (proton transfer comprises the rest of the products), while HO^- reacts with a rate coefficient of $(28 \pm 2) \times 10^{-10}$ cm^3 molecule^{-1} s^{-1} and produces the acetate ion in 78% yield. The acetate ion can be formed *via* $B_{AC}2$ or $B_{AL}2$ mechanisms, but the major pathway is more likely to be $B_{AC}2$ since this product channel is seen for H_2N^-.

The most interesting reaction with methyl acetate occurs with F^- as the nucleophile. In this reaction, five primary products are formed. Two of these products, $FC(=O)CH_2^-$ (36%) and $F^-(CH_3OH)$ (14%), occur from addition to the carbonyl carbon followed by subsequent fragmentation to form $FC(=O)CH_3$ and CH_3O^-. The $FC(=O)CH_2^-$ ion is generated when a proton transfer occurs within the ion–molecule complex, while the $F^-(CH_3OH)$ cluster ion is formed when the proton transfer leads to an elimination reaction to form neutral ketene. Two other products are acetate ion (21%), formed *via* $B_{AL}2$, and the deprotonation product (14%). This reaction is also the only case of the acyclic esters studied here to yield an adduct (14% yield), and this product may be a tetrahedral intermediate or a loose ion–molecule complex between F^- and the alkyl groups of the ester. Previous ICR experiments by Riveros and co-workers have seen only two major products ($FC(=O)CH_2^-$ and $CH_3CO_2^-$), and their reported rate is much slower than our results (by a factor of ~10).[5a,27] Perhaps the different pressure regimes between the corresponding ICR and FA experiments are of importance, and such investigations are in process.

The ionic products, $FC(=O)CH_2^-$ and $F^-(CH_3OH)$, which are produced by the $B_{AC}2$ pathway, are generated even more efficiently at higher temperatures (Table 5), but the overall reaction rate is essentially constant across the temperature regime. This demonstrates that the $B_{AC}2$ pathway becomes more accessible with increasing temperature and suggests that a small barrier may exist for traversing the $B_{AC}2$ mechanism.

Reactions of ethyl acetate

As in the reactions with methyl acetate, the dominant products with ethyl acetate are derived from proton transfer, but the products derived from reaction at the alkyl group also increase. The acetate ion, formed in 31% yield, is now produced for the reaction with H_2N^-, unlike with methyl acetate. The alkyl reaction pathway available to the methyl acetate is *via* $B_{AL}2$ only, but ethyl acetate may also undergo an E2 elimination to yield acetate ion as a product. The increased yield must be due to an E2 pathway. Overall, the reaction rates are quite fast and are very efficient for most of the nucleophiles, except for $NCCH_2^-$.

Another difference between the reactions of methyl and ethyl acetate is that the reaction with methoxide as a nucleophile yields exclusively the $(M–H)^-$ product with methyl acetate, but the $(M–H)^-$ and acetate ions are formed as products with ethyl acetate. The acetate ion product is obviously formed from an E2 reaction at the alkyl group with ethyl acetate.

Finally, the reaction of F^- with ethyl acetate produces only $FC(=O)CH_2^-$ (54%) and $CH_3CO_2^-$ (46%). The former is generated from a $B_{AC}2$ mechanism followed by proton transfer, while the latter is produced from an E2 or a $B_{AL}2$ pathway. The increased reaction rate and efficiency for F^- with ethyl acetate (as compared to methyl acetate) also suggests that the E2 pathway is dominating. Once again, our reaction rate of F^- with ethyl acetate is much faster than reported by Riveros and co-workers in their ICR experiments.[5a,27]

Reactions of β- and γ-lactones

The reactions of β-propiolactone with all of the ions considered here are much faster than the acyclic counterparts, and this is probably due to the faster ADO rates for the lactones (Table 6). However, the chemistry is not very interesting. Most of the observed reactions, except CH_3S^- (see below), are dominated by loss of a proton to yield the $(M–H)^-$ ion. Reactions with γ-butyrolactone also produce the corresponding $(M–H)^-$ ion. Based on the reactions in Table 6, the acidity (ΔH_{acid}) of β-propiolactone appears to be lower than 370 kcal mol^{-1}, but we have not resolved that value any further at this point. It is possible that the products from the lactones are due to elimination reactions to make the corresponding acrylates, and such reactions are known in the condensed phase.[28] We have considered an elimination pathway, but at this point we are unable to distinguish a simple proton transfer from an elimination mechanism as all of our attempts to refine the acidity of the corresponding $(M–H)^-$ ions were unsuccessful. In our current FA apparatus, we did not have enough reaction time to synthesize the ion in question cleanly, and then to characterize its subsequent chemistry.

The only exception to the dominance of proton transfer with these lactones is the reaction of CH_3S^- with β-propiolactone which produces an adduct of some kind. Experiments to determine the nature of the adduct have been attempted. In order to understand if a simple ion–molecule complex was being formed, the reaction was carried out at three different pressures in the hope that the higher pressure would favor complex formation and the reaction rates would increase. However, if there is a pressure dependence, it is within our experimental error (Table 6).

Attempts were made to observe hydrogen–deuterium exchange between the adduct and CD_3OD or CD_3CO_2D, but these studies were not successful. The attempt to determine the acidity of the adduct also met with little success. The adduct would not undergo proton transfer under the time scale of the experiment. The small amount of H/D exchange that was observed was not convincing, but a small amount (~10%) occurs with acetic acid. This signal decrease may actually be the protonation of a reactant and thereby decreases the amount of product seen. The major limitation for these experiments is simply the length of the reaction region (~0.5 m) of our FA as we have to make the reactants, then the adduct ion, and finally study its subsequent chemistry.

Another limitation of our FA is seen in attempts to measure reaction rates with γ-butyrolactone and larger lactones, such as δ-valerolactone and ε-capriolactone. These lactones do not have sufficient vapor pressures at room temperature in order to obtain consistent flow rates of the neutral reagent that is needed to generate accurate kinetic measurements. However, since proton transfer was the only significant channel observed with β-propiolactone and γ-butyrolactone, we did not investigate these reactions any further.

Conclusions

Some interesting trends have been observed. For example, the reactions of $NCCH_2^-$ with the formyl and acetyl esters are dominated by the $B_{AC}2$ mechanism. For reactions with nucleophiles, the ethyl esters typically react faster than the methyl

Table 6 Rates and ionic product distributions for negative ion reactions with lactones[a]

Ion (A^-)	ΔH_{acid} (HA)[b]	*P*/torr	Neutral reagent	Ionic products[c]	Rxn path	Rate[d]	ADO Rate[e]	Eff.[f]
OH^-	391	0.5	β-Propiolactone	$(M–H)^-$	PT	45.0 ± 3.0	41.5	1.00
CH_3O^-	380	0.5	β-Propiolactone	$(M–H)^-$	PT	30.0 ± 2.0	33.1	0.91
F^-	371	0.5	β-Propiolactone	$(M–H)^-$	PT		39.7	
CH_3S^-	357	0.5	β-Propiolactone	CH_3S^-(β-lactone)	Adduct	7.9 ± 0.6	28.9	0.27
		0.8		CH_3S^-(β-lactone)	Adduct	8.2 ± 0.4	28.9	0.28
		1.0		CH_3S^-(β-lactone)	Adduct	8.2 ± 0.6	28.9	0.28
OH^-	391	0.5	γ-Butyrolactone	$(M–H)^-$	PT	12.3 ± 0.3		
CH_3O^-	380	0.5	γ-Butyrolactone	$(M–H)^-$	PT			
$NCCH_2^-$	373	0.5	γ-Butyrolactone	$(M–H)^-$	PT			
$O_2NCH_2^-$	356	0.5	γ-Butyrolactone	No observed reaction				

[a] Rates for the reactions with γ-butyrolactone, δ-valerolactone and ε-capriolactone were tried with little or no success due to vapor pressure problems (see text). [b] Values from the NIST website (http://webbook.nist.gov). [c] %Yields are 100%, extrapolated for a zero flow rate of neutral reagent in STP $cm^3\ s^{-1}$. [d] Rates in units of (10^{-10} cm^3 $molecule^{-1}$ s^{-1}) and the reported errors are one standard deviation of at least triplicate measurements. [e] Rates in units of (10^{-10} cm^3 $molecule^{-1}$ s^{-1}) and the polarizability for β-propiolactone is approximated using group additivity. [f] Efficiency = (experimental rate/ADO rate), and limited to a value of 1.

esters, and the reactivity with the ethyl esters is dominated by chemistry at the alkyl group. This change is due to the availability of the E2 pathway for alkyl reactions with the ethyl esters.[5,24,25]

A comparison of formyl and acetyl esters demonstrates that the formyl esters react more readily with less basic ions, but the rates of reaction of formyl esters with more basic ions are slower than the acetyl esters. The main reason for the increased reaction rate of basic nucleophiles with the acetyl esters is the availability of the proton transfer pathway. The acidity (ΔH_{acid}) of the formyl esters is approximately 391 kcal mol^{-1}, while the acidity of the α-hydrogen in the acetyl esters is approximately 374 kcal mol^{-1}. Other reaction pathways do not compete effectively when proton transfer is favorable (*i.e.* exothermic).

The Riveros pathway dominates the reactivity of methyl formate. The $B_{AC}2$ pathway is observed to only a very small extent with methyl formate as a substrate. F^- ion demonstrates some interesting reactivity with the esters considered here. Computational (B3LYP/6-31+G(d)) results demonstrate that the $B_{AL}2$ pathway (Fig. 5a) has the lowest activation barrier; however, the experimental results at 298 K (Table 5) show a slight preference for the Riveros pathway. The calculated Riveros pathway has a slightly endothermic (+0.3 kcal mol^{-1}) barrier, and variable temperature experimental studies demonstrate an increase in the Riveros product as the temperature is increased from 298 to 448 K.

Moreover, from a mechanistic sense, the Riveros product can be generated through two different routes: a F^--assisted C–O bond cleavage (Fig. 5b) or through nucleophilic attack at the carbonyl carbon ($B_{AC}2$, Fig. 5c). In the $B_{AC}2$ pathway, the alkoxide leaving group abstracts a proton from the formyl or acetyl group prior to departing from the complex.

Further examples of nucleophilic reactivity with carbonyl groups will be presented in due course from both experimental and computational approaches.

Acknowledgements

This research was supported by the National Science Foundation (CHE-9733457). We also acknowledge the donors of the Petroleum Research Fund, administered by the American Chemical Society, for partial support of this research. We also acknowledge support by the Ohio Supercomputer Center where some of these calculations were performed. In addition, we are grateful to the reviewers for many helpful comments.

We are particularly pleased to dedicate this paper to Bob Squires, who was an inspiration and a role model for us. Bob never hesitated to offer his advice, his energy, and his creativity for our flowing afterglow development and for this carbonyl project, in particular. Bob was gifted as a scientist, a teacher, and a friend. Bob made us all better because he was there to help and to guide. We will miss him. Goodbye, Bob.

References

1 (*a*) *The Chemistry of the Carbonyl Group*, S. Patai, Ed., Interscience, New York, 1966; (*b*) J. Falbe, in *Methoden der Organische Chemie (Houben-Weyl)*, G. Thieme Verlag, Stuttgart, 1983, Vol. E3; E. Muller, in *Methoden der Organische Chemie (Houben-Weyl)*, G. Thieme Verlag, Stuttgart, 1973, Vol. 7/7; (*c*) M. L. Bender, *J. Am. Chem. Soc.*, 1951, **73**, 1626; (*d*) M. L. Bender, *Chem. Rev.*, 1960, **60**, 53; (*e*) W. P. Jencks, *Prog. Phys. Org. Chem.*, 1964, **2**, 63; (*f*) A. J. Parker, *Chem. Rev.*, 1969, **69**, 1; (*g*) E. H. Cordes and H. G. Bull, *Chem. Rev.*, 1974, **74**, 581; (*h*) W. P. Jencks, *Acc. Chem. Res.*, 1980, **13**, 161.

2 (*a*) K. B. Wiberg, C. M. Hadad, P. R. Rablen and J. Cioslowski, *J. Am. Chem. Soc.*, 1992, **114**, 8644; (*b*) K. B. Wiberg and P. R. Rablen, *J. Am. Chem. Soc.*, 1995, **117**, 2201; (*c*) C. M. Hadad, P. R. Rablen and K. B. Wiberg, *J. Org. Chem.*, 1998, **63**, 8668.

3 (*a*) G. D. Paderas, P. Metivier and W. L. Jorgensen, *J. Org. Chem.*, 1991, **56**, 4718; (*b*) R. A. J. O'Hair, G. E. Davico, J. Hacaloglu, T. T. Dang, C. H. DePuy and V. M. Bierbaum, *J. Am. Chem. Soc.*, 1994, **116**, 3609; (*c*) S. T. Arnold, R. A. Morris and A. A. Viggiano, *J. Chem Phys.*, 1995, **103**, 9242; (*d*) J. V. Seeley, R. A. Morris and A. A. Viggiano, *J. Phys. Chem.*, 1996, **100**, 15821; (*e*) S. T. Arnold, R. A. Morris, A. A. Viggiano and M. A. Johnson, *J. Phys. Chem.*, 1996, **100**, 2900.

4 (*a*) O. I. Asubiojo, L. K. Blair and J. I. Brauman, *J. Am. Chem. Soc.*, 1975, **97**, 6685; (*b*) O. I. Asubiojo and J. I. Brauman, *J. Am. Chem. Soc.*, 1979, **101**, 3715; (*c*) J. L. Wilbur and J. I. Brauman, *J. Am. Chem. Soc.*, 1994, **116**, 5839; (*d*) J. L. Wilbur and J. I. Brauman, *J. Am. Chem. Soc.*, 1994, **116**, 9216.

5 (*a*) J. M. Riveros, S. M. Jose and K. Takashima, *Adv. Phys. Org. Chem.*, 1985, **21**, 197; (*b*) J. M. Riveros, *J. Chem. Soc., Chem. Commun.*, 1990, 773.

6 (*a*) J. D. Baldeschweiler and S. S. Woodgate, *Acc. Chem. Res.*, 1971, **4**, 114; (*b*) M. Comisarow, *Can. J. Chem.*, 1977, **55**, 171; (*c*) C. H. DePuy, J. J. Grabowski, V. M. Bierbaum, S. Ingemann and N. M. M. Nibbering, *J. Am. Chem. Soc.*, 1985, **107**, 1093; (*d*) N. M. M. Nibbering, *Acc. Chem. Res.*, 1990, **23**, 279; (*e*) C. F. Bernasconi, M. W. Stronach, C. H. DePuy and S. Gronert, *J. Am. Chem. Soc.*, 1990, **112**, 9044.

7 (*a*) E. E. Ferguson, F. C. Fehsenfeld and A. L. Schmeltekopf, *Adv. At. Mol. Phys.*, 1969, **5**, 1; (*b*) C. H. DePuy and V. M. Bierbaum, *Acc. Chem. Res.*, 1981, **14**, 146.

8 (*a*) N. G. Adams and D. Smith, *Int. J. Mass Spectrom. Ion Phys.*, 1976, **21**, 349; (*b*) J. M. Van Doren, S. E. Barlow, C. H. DePuy and V. M. Bierbaum, *Int. J. Mass Spectrom. Ion Proc.*, 1987, **81**, 85.

9 S. T. Graul and R. R. Squires, *J. Am. Chem. Soc.*, 1990, **112**, 2517.

10 M. McFarland, D. L. Albritton, F. C. Fehsenfeld, E. E. Ferguson and A. L. Schmeltekopf, *J. Chem. Phys.*, 1973, **59**, 6610.

11 (*a*) D. B. Dunkin, F. C. Fehsenfeld, A. L. Schmeltekopf and E. E. Ferguson, *J. Chem. Phys.*, 1968, **49**, 1365; (*b*) S. R. Kass, H. Guo and G. D. Dahlke, *J. Am. Soc. Mass Spectrom.*, 1990, **1**, 366; (*c*) B. T. Frink, PhD Thesis, The Ohio State University, 1999.

12 S. T. Graul and R. R. Squires, *Mass Spectrom. Rev.*, 1988, **7**, 263.
13 (*a*) J. F. G. Faigle, P. C. Isolani and J. M. Riveros, *J. Am. Chem. Soc.*, 1976, **98**, 2049; (*b*) K. Takashima and J. M. Riveros, *J. Am. Chem. Soc.*, 1978, **100**, 6128.
14 J. E. Bartmess, R. L. Hays and G. Caldwell, *J. Am. Chem. Soc.*, 1981, **103**, 1338.
15 (*a*) J. D. Madura and W. L. Jorgensen, *J. Am. Chem. Soc.*, 1986, **108**, 2517; (*b*) J. F. Blake and W. L. Jorgensen, *J. Am. Chem. Soc.*, 1987, **109**, 3856.
16 R. E. Rosenberg, *J. Am. Chem. Soc.*, 1995, **117**, 10358.
17 M. Zhong and J. I. Brauman, *J. Am. Chem. Soc.*, 1999, **121**, 2508.
18 I. Lee, D. Lee and C. K. Kim, *J. Phys. Chem. A*, 1997, **101**, 879.
19 J. J. Grabowski and L. Zhang, *J. Am. Chem. Soc.*, 1989, **111**, 1193.
20 GAUSSIAN94, Revision D.3: M. J. Frisch, G. W. Trucks, H. B. Schlegel, P. M. W. Gill, B. G. Johnson, M. A. Robb, J. R. Cheeseman, T. Keith, G. A. Petersson, J. A. Montgomery, K. Raghavachari, M. A. Al-Laham, V. G. Zakrzewski, J. V. Ortiz, J. B. Foresman, J. Cioslowski, B. B. Stefanov, A. Nanayakkara, M. Challacombe, C. Y. Peng, P. Y. Ayala, W. Chen, M. W. Wong, J. L. Andres, E. S. Replogle, R. Gomperts, R. L. Martin, D. J. Fox, J. S. Binkley, D. J. Defrees, J. Baker, J. P. Stewart, M. Head-Gordon, C. Gonzalez and J. A. Pople, Gaussian, Inc., Pittsburgh, PA, 1995.
21 (*a*) T. Ziegler, *Chem. Rev.*, 1991, **91**, 651; (*b*) *Density Functional Methods in Chemistry*, J. Labanowski and J. Andzelm, Eds., Springer-Verlag, New York, 1991; (*c*) R. G. Parr and W. Yang, *Density-Functional Theory of Atoms and Molecules*, Oxford University Press, New York, 1989; (*d*) A. D. Becke, *J. Chem. Phys.*, 1993, **98**, 5648; (*e*) C. Lee, W. Yang and R. G. Parr, *Phys. Rev. B*, 1988, **37**, 785; (*f*) P. J. Stephens, F. J. Devlin and M. J. Frisch, *J. Phys. Chem.*, 1994, **98**, 11623; (*g*) B. G. Johnson, P. M. W. Gill and J. A. Pople, *J. Chem. Phys.*, 1993, **98**, 5612; (*h*) W. Hehre, L. Radom, P. v. R. Schleyer and J. A. Pople, *Ab initio Molecular Orbital Theory*, John Wiley & Sons, New York, 1986.
22 (*a*) C. Gonzalez and H. B. Schlegel, *J. Chem. Phys.*, 1989, **90**, 2154; (*b*) C. Gonzalez and H. B. Schlegel, *J. Phys. Chem.*, 1990, **94**, 5523.
23 T. Su and M. T. Bowers, *Int. J. Mass Spectrom. Ion Phys.*, 1973, **12**, 347.
24 C. H. DePuy, S. Gronert, A. Mullin and V. M. Bierbaum, *J. Am. Chem. Soc.*, 1990, **112**, 8650 and references therein.
25 (*a*) C. H. DePuy and V. M. Bierbaum, *J. Am. Chem. Soc.*, 1981, **103**, 5034; (*b*) C. H. DePuy, E. C. Beedle and V. M. Bierbaum, *J. Am. Chem. Soc.*, 1982, **104**, 6483; (*c*) V. M. Bierbaum, J. Filley, C. H. DePuy, M. F. Jarrold and M. T. Bowers, *J. Am. Chem. Soc.*, 1985, **107**, 2818; (*d*) S. Gronert, C. H. DePuy and V. M. Bierbaum, *J. Am. Chem. Soc.*, 1991, **113**, 4009.
26 B. T. Frink, C. M. Geise and C. M. Hadad, unpublished results.
27 S. M. José and J. M. Riveros, *Nouv. J. Chim.*, 1977, **1**, 113.
28 J. Mulzer and T. Kerkmann, *J. Am. Chem. Soc.*, 1980, **102**, 3620.

Paper 9/05632G